Title

Syntaxin13 Expression Is Regulated by Mammalian Target of Rapamycin (mTOR) in Injured Neurons to Promote Axon Regeneration*

Authors

Cho, Yongcheol
Di Liberto, Valentina
Carlin, Dan
et al.

Syntaxin13 Expression Is Regulated by Mammalian Target of Rapamycin (mTOR) in Injured Neurons to Promote Axon Regeneration[*]

Yongcheol Cho[‡1], **Valentina Di Liberto**[‡1,2], **Dan Carlin**[‡], **Namiko Abe**[‡3], **Kathy H. Li**[§], **Alma L. Burlingame**[§], **Shenheng Guan**[§], **Izhak Michaelevski**[¶], and **Valeria Cavalli**[‡4]

From the [‡]Department of Anatomy and Neurobiology, Washington University in St Louis, School of Medicine, St. Louis, Missouri 63110, the [§]Mass Spectrometry Facility, Department of Pharmaceutical Chemistry, University of California at San Francisco, San Francisco, California 94158-2517, and the [¶]Department of Biochemistry and Molecular Biology, Tel Aviv University, Tel Aviv 69978, Israel

Background: Axon regeneration following nerve injury depends on activation of mTOR.
Results: Nerve injury increases the expression of syntaxin13 in an mTOR-dependent manner.
Conclusion: Injury-induced synthesis of syntaxin13 is important for axon regeneration.
Significance: Learning which proteins are synthesized via mTOR in injured nerves is crucial to our understanding of regenerative mechanisms in peripheral neurons.

Injured peripheral neurons successfully activate intrinsic signaling pathways to enable axon regeneration. We have previously shown that dorsal root ganglia (DRG) neurons activate the mammalian target of rapamycin (mTOR) pathway following injury and that this activity enhances their axon growth capacity. mTOR plays a critical role in protein synthesis, but the mTOR-dependent proteins enhancing the regenerative capacity of DRG neurons remain unknown. To identify proteins whose expression is regulated by injury in an mTOR-dependent manner, we analyzed the protein composition of DRGs from mice in which we genetically activated mTOR and from mice with or without a prior nerve injury. Quantitative label-free mass spectrometry analyses revealed that the injury effects were correlated with mTOR activation. We identified a member of the soluble *N*-ethylmaleimide-sensitive factor attachment protein receptor (SNARE) family of proteins, syntaxin13, whose expression was increased by injury in an mTOR-dependent manner. Increased syntaxin13 levels in injured nerves resulted from local protein synthesis and not axonal transport. Finally, knockdown of syntaxin13 in cultured DRG neurons prevented axon growth and regeneration. Together, these data suggest that syntaxin13 translation is regulated by mTOR in injured neurons to promote axon regeneration.

Recovery from a peripheral nerve injury can be relatively successful because the injured neurons activate intrinsic signaling pathways to enable axon regeneration (1). Defining the signaling pathways and protein ensembles that are up-regulated after injury will not only provide new information on regenerative growth but also support novel approaches to promote functional recovery following nerve injury.

Initially described as chromatolysis or cell body reaction, injury to peripheral nerves triggers a series of morphologic and biochemical changes in neuronal cell bodies (2, 3), including increases in RNA content and in the rate of protein synthesis (4, 5). The molecular mechanisms controlling the protein synthesis machinery include the evolutionarily conserved mammalian target of rapamycin (mTOR),[5] which integrates upstream signals to control cellular growth and proliferation. Previously, we showed that peripheral nerve injury robustly and transiently activates mTOR and that blocking mTOR activity pharmacologically reduces axon growth ability (6). Activating the mTOR pathway by genetically silencing its negative regulators, such as TSC2 in sensory neurons (6) or PTEN or TSC1 in adult CNS neurons (7, 8), results in extensive axon regeneration. These studies indicate that mTOR-dependent increase in protein synthesis contributes to axon regeneration. Protein synthesis localized in axons also plays a crucial role in promoting regenerative growth by promoting growth cone formation and initiating the retrograde transport of injury signals (9, 10). Together, these studies demonstrate that increased protein synthesis is linked to the ability of neurons to regenerate.

Given the importance of protein synthesis for axon regeneration, here we used a mass spectrometry approach to identify proteins whose expression is regulated by injury in an mTOR-dependent manner and to play a role in regenerative growth. We analyzed the protein composition of dorsal root ganglia

(DRG) neurons from mice in which we genetically activated mTOR and from control mice with or without a prior injury. Using semiquantitative proteomics, we show that the effect of injury correlates with the effect of genetic mTOR activation. We identified syntaxin13 as a protein whose expression is increased by injury in an mTOR-dependent manner. Syntaxin13 is an integral membrane protein belonging to the t-SNARE family, a group of proteins involved in membrane fusion. Syntaxin13 plays a role in endosomal recycling of plasma membrane constituents (11) and the formation of lamellipodia during cell adhesion (12). Overexpression of syntaxin13 enhances neurite outgrowth in PC12 cells (13), suggesting that a syntaxin13-dependent endocytic trafficking step plays a role in neuronal development. We found that syntaxin13 levels were locally enhanced in the injured nerve via local protein synthesis, and knockdown of syntaxin13 in cultured DRG neurons markedly reduced axon growth and regeneration. Together, these data suggest that mTOR activity enhances syntaxin13 expression in injured nerves to promote axon regeneration.

EXPERIMENTAL PROCEDURES

Antibodies, Reagents, and Lentiviruses—The following antibodies were used: anti-tuberin/TSC2 (C terminus, Santa Cruz Biotechnology); anti-α-tubulin (Abcam); anti-syntaxin13 (Synaptic Systems); anti-phosphorylated S6 ribosomal protein (serine 240/244, Cell Signaling), and anti-APP (N terminus, Millipore). Syntaxin13 cDNA was received from H. Hirling (13) and cloned into FUGW lentiviral vector to express the fusion protein GFP-syntaxin13. To knock down syntaxin13 without targeting recombinant GFP-syntaxin13, we used a mouse shRNA sequence targeting the syntaxin13 3′UTR (CCTGGCTTT-GATGGCAAGATT). shRNA lentivirus was produced using pLKO.1 constructs from The RNAi Consortium following the manufacturer's manual.

Animals—For experiments involving wild-type animals, C57B6 6–9-month-old females were used. TSC2 conditional knockouts were obtained by crossing *Tsc2$^{flox/flox}$* animals with *Advil-lin$^{Cre/Cre}$*, as described previously (6). Genotypes were confirmed by tail PCR at weaning age. Littermate controls were used for all experiments.

Surgical Procedures, Drug Treatment, and Sample Preparation—All surgical procedures were approved by the Washington University in St. Louis, School of Medicine Animal Studies Committee. Sciatic nerve injury experiments were performed as described previously (15). Briefly, the sciatic nerves of mice were ligated unilaterally at the midpoint, and mice were sacrificed at the indicated time after surgery. Rapamycin was delivered by intraperitoneal injection at 5 mg/kg body weight. Rapamycin was dissolved in 200 μl of DMEM from a 10 mg/ml stock solution in dimethyl sulfoxide. An equivalent volume of dimethyl sulfoxide was dissolved into 200 μl of DMEM for vehicle control. Intraperitoneal injection was performed 1 h before sciatic nerve ligation. Animals were sacrificed, and DRGs and nerves were dissected 24 h following ligation. For other chemical treatments, sciatic nerves were soaked with chemicals dissolved in DMSO in Surgifoam (Johnson & Johnson) 30 min prior to injury as described (15). Drug concentrations were as follows: cycloheximide, 1 mM, 100 μl; nocodazole, 0.33 mM, 100 μl.

For biochemical studies on DRG cell bodies, L4 and L5 DRGs were dissected from both the injured side and the control contralateral uninjured side. For biochemistry on the sciatic nerve, equal lengths (3 mm) of the proximal and distal parts were homogenized in lysis buffer (20 mM Tris-HCl, pH 7.5, 150 mM NaCl, 1 mM Na$_2$EDTA, 1 mM EGTA, 1% Triton X-100, 2.5 mM sodium pyrophosphate, 1 mM β-glycerophosphate, 1 mM Na$_3$VO$_4$, 1 μg/ml leupeptin) with phosphatase inhibitor mixtures 1 and 2 (Invitrogen). DRGs were also lysed in this buffer. Equal protein amounts (10 μg) were loaded and analyzed by SDS-PAGE and Western blot.

For immunohistochemistry, mouse sciatic nerves were dissected, fixed in 4% paraformaldehyde in PBS for 1 h, incubated overnight in 30% sucrose in PBS, embedded in OCT solution (Tissue-Tek), and frozen in dry ice-cooled methylbutane. Longitudinal sections of fixed sciatic nerves were stained with syntaxin13 antibodies.

Mass Spectrometry Analysis—Protein samples (5 μg) of DRG extracts were separated by SDS-PAGE and stained with Coomassie, and the gel lanes were then sliced into nine different pieces. Each gel piece was digested with trypsin, and the resulting peptides were analyzed using the LC-MS/MS method on an Orbitrap XL instrument (ThermoFisher Scientific, Bremen, Germany), interfaced with a NanoAcquity LC system (Waters). Survey scans were acquired in the Orbitrap MS using a mass resolution of 60,000. Six MS/MS scans were acquired in the ion trap for each survey scan.

Peptide identification was obtained by use of an in-house Protein Prospector search engine (16, 17). The search parameters included the following: enzyme specificity = trypsin; allowed missed cleavages = 1; fixed modification = carbamidomethylation; variable modifications = acetylation on protein N terminus, glutamine on peptide N-terminal to glutamic acid, methionine loss from protein N terminus, methionine loss from protein N terminus and acetylation, methionine oxidation, serine and threonine phosphorylation; maximal number of variable modifications = 2; parent mass tolerance = 20 ppm; fragment mass tolerance = 0.6 Da; peptide expectation cutoff = 0.05. The match of the decoy database sequences indicated that the false discovery rate for the expectation cutoff value is about 0.09%.

Label-free quantification was performed using an extracted ion chromatogram algorithm. We adapted a label-free quantification portion of a data processing pipeline developed for protein turnover studies (18). For particular peptides of interest, manual extraction of ion chromatograms was performed using the instrument software (Xcalibur from ThermoFisher Scientific, San Jose, CA).

Proteomic Data Analysis and Clustering—Proteomic data were further analyzed using hierarchic cluster analyses via Euclidean metrics for distance assessment and Ward minimum variance for linkage (19, 20). For subclustering reasons, we used an average linkage algorithm. Amalgamation curves were employed to estimate cluster number and to supervise reclustering. At each step of the hierarchic clustering, the data were validated using the root mean square deviation of the cluster,

and pseudo-*F* ratio, pseudo *T*-square estimation, and Dunn's cluster separation maximum group assessment methods. For gene ontology, we used the David bioinformatics server tool with the following parameters: medium classification stringency, κ similarity = 3; final group membership of at least 3; and enrichment threshold 1.0; out of 9 gene ontology clusters revealed, four clusters satisfied the 1.0 enrichment threshold (vesicle associate protein, score 3.19; nucleotide biosynthesis-related cluster, score 1.66; endoplasmic reticulum-associated proteins, score 1.16; nucleotide-binding proteins, score 1.09); however, only the first cluster, vesicle associate protein, met the false discovery rate threshold 5% requirement analysis.

DRG Culture, in Vitro Axotomy, and Regeneration Assays—Mouse embryonic DRG spot cultures, *in vitro* axotomy, and regeneration assays were performed as described previously (15). Briefly, embryonic E13.5 DRGs were dissociated and plated in a defined region with 10^4 cells/2.5 μl. Culture medium was added 10 min after plating. DRG neurons were axotomized using a blade (FST, 10035-10) at DIV7. For determination of syntaxin13 levels in injured axons, vehicle or cycloheximide was applied for 1 h prior to axotomy, and DRG neurons were fixed and stained for βIII-tubulin and syntaxin13 3 h after axotomy. The ratio of fluorescence intensity between syntaxin13 and βIII-tubulin was measured using ImageJ. For *in vitro* regeneration assay, DRG neurons were fixed 0 or 40 h after axotomy and stained for βIII-tubulin. Axons were visualized by fluorescence with a $\times$10 objective (Nikon, TE2000E). A regeneration index was calculated from the images acquired 40 h post axotomy (15). Briefly, the fluorescence intensity of a square area $(2.7 \times 0.1 \text{ mm})$ at 0.1 mm distal to the axotomy line was measured and normalized to the similar area 0.1 mm proximal to the axotomy line. The number of regenerating axons crossing the axotomy line was measured using ImageJ.

Statistics—Western blots were scanned and quantified by ImageJ, and the *t* test was used for statistical analysis. For multiple comparisons, analysis of variance followed by Tukey tests and *t* tests were used.

RESULTS

Changes in Protein Expression Induced by Nerve Injury Correlate with Those Regulated by Genetic mTOR Activation—Previously, we showed that DRG neurons activate mTOR following injury, and this activity enhances axon growth capacity (6). Genetic up-regulation of mTOR activity by deletion of the negative regulator TSC2 in DRGs is sufficient to enhance axon growth capacity (6). mTOR-dependent increase in protein synthesis led to the up-regulation of the growth-associated protein GAP-43 in injured sensory nerves (6). It seems likely that the mTOR pathway regulates the translation of a number of other proteins to maximize axon growth capacity. Hence, to identify proteins associated with regenerative growth, we compared the DRG proteome from mice in which we genetically activated mTOR in DRG neurons or from mice that received a sciatic nerve injury 4 days prior to DRG dissection. In theory, the potential convergence of an injury-related signaling pathway on mTOR activation should create similar protein expression patterns in naive neurons lacking TSC2 and injured WT neurons. To genetically activate mTOR in DRG neurons, we

deleted TSC2 in sensory neurons by crossing $Tsc2^{flox/flox}$ mice to $Advillin^{Cre/Cre}$, generating $Tsc2^{flox/flox}$;Advillin$^{Cre/+}$ conditional knock-out animals, hereafter referred to as TSC2KO (6). Injury-induced activation of mTOR in wild-type (WT) mice was achieved by performing a sciatic nerve ligation 4 days prior to DRG dissection. We chose this time point because 4 days is sufficient to promote the conditioning injury effect as well as to enhance axon growth capacity (6). We then prepared DRG extracts, separated proteins by SDS-PAGE, and performed in-gel digest with trypsin. Peptides were analyzed by nanoLC-MS/MS. Approximately 2700 proteins were identified in each sample. We performed automated label-free quantification by using the mean peak area ratio as a measure of relative protein abundance.

We then conducted correlative and cluster analyses between protein expression patterns in TSC2KO *versus* noninjured WT (WT−), as well as in injured WT (WT+) *versus* WT−. Because mass spectrometry analysis identified different numbers of proteins in WT−, TSC2KO, and WT+ groups, we retained only those proteins that were detected in both analytical groups for evaluation, leading to 236 proteins for each group. Analysis of the standard deviation distribution profile for each protein indicated that there were less than 5% outliers beyond two standard deviations for the proteins found in all groups. Pearson's correlation analysis revealed a prominent all point positive correlation between the evaluated groups ($r = 0.6$) that was reflected in an all point histogram and corresponding probability density functions (Fig. 1*A*). Per point analyses revealed significant deviations between protein expression patterns in WT+/WT− and TSC2KO/WT− groups (Fig. 1*B*). Hierarchic clustering analysis was then conducted to pinpoint the proteins exhibiting the highest similarity in expression pattern between WT+/WT− and TSC2KO/WT− (Fig. 1*C*). Using this strategy, 10 clusters were enriched, which passed validation algorithms for the hierarchic clustering approach. Most of the clusters revealed a similar behavior pattern, and the resemblance was particularly prominent for clusters 1, 2, 4, 6, 7, and 9. To further decrease the list of proteins being up- and down-regulated in a similar fashion between WT+/WT− and TSC2KO/WT− pairs, we set a threshold of ±0.5-fold logarithmic scale change (base of 2). This threshold corresponded to about 41% up-regulation and 29% down-regulation of protein expression in WT+/WT− and TSC2KO/WT− pairs. These magnitudes of change were found to be statistically significant using one sample one tail *t* test analysis. Thirty five down-regulated proteins (clusters 1, 3, and 4; Table 1) and 23 up-regulated proteins (clusters 6, 7, and 8; Table 2) passed the threshold of $\log_2$(protein ratio) = ±0.5. Further re-clustering of the down-regulated proteins revealed four subclusters with a high similarity of behavior in subclusters 1 and 3 (Fig. 1*E*). Re-clustering of the up-regulated proteins revealed the existence of two uneven sized clusters (Fig. 1*D*).

Although most clusters failed to be enriched to a specific gene ontology category, one down-regulated protein subcluster exhibited functional association with vesicle turnover impairment. Furthermore, we found that the expression of RhoA, a small GTPase known for its role in growth cone collapse and outgrowth failure (21), was down-regulated in both WT+/
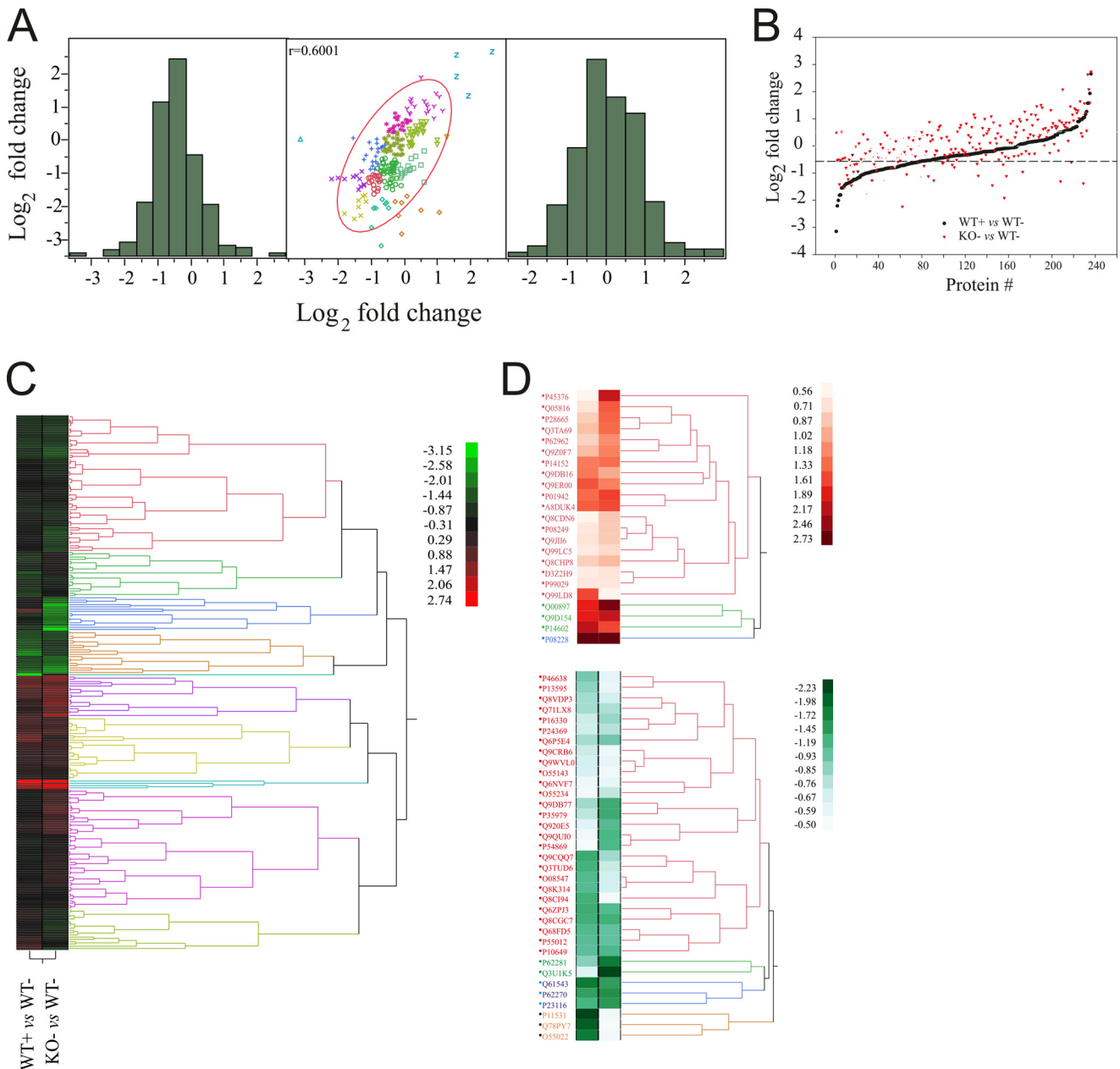
FIGURE 1. **Protein expression pattern induced by nerve injury correlates with those regulated by genetic mTOR activation.** *A,* correlation of protein expression pattern changes between noninjured WT (*WT−*) and injured WT (*WT+*) and TSC2KO/WT− pairs. *Left panel,* all point histogram of protein expression level changes for WT+/WT−. *Middle panel,* Pearson's pairwise correlation analysis. *Right panel,* all point histogram of protein expression level changes for TSC2KO/WT−. *r* denotes correlation coefficient. All point color distribution and symbol assignment correspond to their subcluster as shown on *C. B,* protein level fold change analysis of TSC2KO/WT− (*red dots*) *versus* WT+/WT− (*black dots*). The distribution shows the changes of a particular protein between two pairs. *C,* hierarchic cluster analysis of protein expression pattern change in WT+/WT− and TSC2KO/WT− pairs. *D,* hierarchic cluster analysis applied to enriched up- and down-regulated clusters (see in text) in WT+/WT− and TSC2KO/WT− pairs. The *upper* and *lower panels* depict differentially up- and down-regulated clusters, respectively.

WT− and TSC2KO/WT− comparison groups. Analysis of the up-regulated proteins showed that the enhancement of protein expression was very limited in both WT+/WT− and TSC2KO/WT− comparison groups. This relatively limited enhancement in protein expression could result from the complexity of DRG tissue, containing neurons and non-neuronal cells as well as connective tissue, which decreases the sensitivity of our proteomics analysis and thus limit the identification of low abundant neuronal protein. Nevertheless, a close analysis of two enriched clusters in the up-regulated proteins groups revealed

that two proteins, the SNARE protein syntaxin13 and superoxide dismutase, were increased in both WT+/WT− and TSC2KO/WT− comparison groups. This analysis indicates that genetic activation of mTOR leads to changes in protein expression in DRG that partially overlap with those induced by a prior nerve injury.

Genetic mTOR Activation in Sensory Neurons Increases Syntaxin13 Levels—We decided to focus our study on syntaxin13 because this protein plays a role in neurite outgrowth in PC12 cells (13). Furthermore, syntaxin13 localizes to the recycling

TABLE 1

List of down-regulated proteins

Cluster analysis of differentially down-regulated proteins corresponds to Fig. 1D, *lower panel*. log2(protein ratio) = −0.5 was used as down-regulation threshold. Data are represented using Uniprot accession number, gene symbol IDs, full name of the genes, number of peptides used for protein reconstruction, protein fold changes with standard deviation, and cluster ID number. Data have been sorted according to amalgamation curve of occurrence in assigned clusters.

Swiss Prot.	Protein Name	Pep. #	AVE_Log(WT+/WT−)	STDEV_Log(WT+/WT−)	Pep. #	AVE_Log(KO−/WT−)	STDEV_Log(KO−/WT−)	Gene Symbol	Cluster
P46638	Ras-related protein Rab-11B	5	−1.07	0.42	5	−0.61	0.66	*Rab11B*	1
P13595	Neural cell adhesion molecule 1	6	−0.99	0.50	5	−0.57	0.27	*Ncam1*	1
Q8VDP3	NEDD9-interacting protein with calponin homology and LIM domains	4	−0.93	0.20	4	−0.68	1.17	*Mical1*	1
Q71LX8	Heat shock protein 84b	16	−0.93	0.73	17	−0.78	0.68	*HSP90AB1*	1
Q6P5E4	UDP-glucose:glycoprotein glucosyltransferase 1	3	−0.92	0.76	3	−0.91	0.74	*Uggt1*	1
P16330	2′,3′-cyclic-nucleotide 3′-phosphodiesterase	9	−0.81	0.49	5	−0.82	0.41	*Cnp*	1
Q9CRB6	Tubulin polymerization-promoting protein family member 3	4	−0.81	0.83	5	−0.54	1.91	*Tppp3*	1
P24369	Peptidyl-prolyl cis-trans isomerase B	4	−0.80	0.22	3	−0.76	0.07	*PpiB*	1
Q9WVL0	Maleylacetoacetate isomerase	3	−0.77	0.30	3	−0.59	0.42	*Gstz1*	1
O55143	Sarcoplasmic/endoplasmic reticulum calcium ATPase 2	13	−0.74	0.76	6	−0.54	0.90	*ATP2A2*	1
Q6NVF7	Prx protein	11	−0.60	0.50	15	−0.58	0.82	*Prx*	1
O55234	Proteasome subunit beta type-5	4	−0.55	0.36	5	−0.74	0.30	*Psmb5*	1
Q9DB77	Cytochrome b-c1 complex subunit 2, mitochondrial	7	−0.95	0.45	4	−1.27	0.38	*Uqcrc2*	1
P35979	60S ribosomal protein L12	4	−0.86	0.41	5	−1.28	0.49	*rpl12*	1
Q920E5	Farnesyl pyrophosphate synthase	3	−0.68	0.56	3	−1.05	1.28	*Fdps*	1
Q9QUI0	Transforming protein RhoA	3	−0.57	0.23	3	−1.15	0.98	*Rhoa*	1
P54869	Hydroxymethylglutaryl-CoA synthase, mitochondrial	5	−0.53	0.48	4	−1.12	0.44	*Hmgcs2*	1
Q9CQQ7	ATP synthase subunit b, mitochondrial	6	−1.40	0.32	6	−0.81	0.41	*Atp5f1*	1
Q6ZPJ3	Ubiquitin-conjugating enzyme E2 O	5	−1.39	0.54	4	−1.07	0.25	*Ube2o*	1
Q8CGC7	Bifunctional aminoacyl-tRNA synthetase	8	−1.37	0.85	9	−1.22	0.89	*Eprs*	1
Q8CI94	Glycogen phosphorylase, brain form	6	−1.35	0.09	9	−0.51	0.48	*Pygb*	1
Q3TUD6	Putative uncharacterized protein	9	−1.34	0.56	8	−0.72	0.67	*Hsp90b1*	1
Q68FD5	Clathrin heavy chain 1	15	−1.24	0.64	16	−0.95	0.73	*Cltc*	1
O08547	Vesicle-trafficking protein SEC22b	4	−1.24	0.27	3	−0.68	0.27	*Sec22b*	2
Q8K314	Atp2b1 protein (Fragment)	7	−1.21	0.49	5	−0.66	0.74	*Atp2b1*	2
P55012	Solute carrier family 12 member 2	3	−1.18	0.39	4	−0.94	0.47	*Slc12a2*	3
P10649	Glutathione S-transferase Mu 1	5	−1.15	0.34	3	−1.10	0.89	*Gstm1*	3
P62281	40S ribosomal protein S11	5	−1.01	1.07	3	−1.77	0.08	*Rps11*	3
Q3U1K5	Advillin	7	−0.72	0.55	3	−2.24	0.40	*Avil*	3
Q61543	Golgi apparatus protein 1	6	−1.81	0.54	4	−1.41	0.18	*Glg1*	3
P62270	40S ribosomal protein S18	4	−1.50	1.15	4	−1.54	0.29	*Rsp18*	3
P23116	Eukaryotic translation initiation factor 3 subunit A	4	−1.31	0.69	5	−1.46	0.57	*Eif3a*	3
P11531	Dystrophin	4	−2.21	0.56	5	−0.53	0.37	*Dmd*	4
Q78PY7	Staphylococcal nuclease domain-containing protein 1	6	−2.01	0.60	10	−0.50	0.61	*Snd1*	4
O55022	Membrane-associated progesterone receptor component 1	3	−1.81	1.93	4	−0.52	0.27	*Pgrmc1*	4

TABLE 2

List of up-regulated proteins

Cluster analysis of differentially up-regulated proteins correspond to Fig. 1D, *upper panel.* log2(protein ratio) = +0.5 was used as up-regulation threshold. Data are represented using Uniprot accession number, gene symbol IDs, and full name of the genes, number of peptides used for protein reconstruction, protein fold changes with standard deviation, and cluster ID number. Data have been sorted according to amalgamation curve of occurrence in assigned clusters

Swiss Prot	Protein Name	Pep. #	AVE_Log(WT+/WT-)	STDEV_Log(WT+/WT-)	Pep. #	AVE_Log(KO/WT-)	STDEV_Log(KO/WT-)	Gene Symbol	Cluster
P45376	Aldose reductase	5	0.50	0.23	6	2.08	0.39	Akr1b3	1
Q05816	Fatty acid-binding protein, epidermal	3	0.58	0.04	3	1.46	0.41	Fabp5	1
P62962	Profilin-1	6	0.65	0.23	6	1.15	0.28	Pfn1	1
P28665	Murinoglobulin-1	3	0.67	0.67	5	1.38	0.50	Mug1	1
Q3TA69	Putative uncharacterized protein	3	0.70	0.55	3	1.33	0.30	LOC100047ε	1
Q9Z0F7	Gamma-synuclein	7	0.71	0.50	10	1.22	0.59	Sncg	1
P14152	Malate dehydrogenase, cytoplasmic	5	0.90	0.62	7	1.31	0.74	Mdh1	1
Q9DB16	Calcium-binding protein 39-like	4	0.90	0.39	3	1.02	0.16	Cab39l	1
P01942	Hemoglobin subunit alpha	5	0.95	0.58	3	1.64	0.31	Hba-a1	1
A8DUK4	Beta-globin	7	1.05	1.19	6	1.57	3.38	Hbb-b2	1
Q9ER00	Syntaxin-12	2	1.16	0.17	2	1.22	0.67	Stx12	1
Q8CDN6	Thioredoxin-like protein 1	3	0.50	0.81	3	0.87	0.48	Txnl1	1
Q99LC5	Electron transfer flavoprotein subunit alpha, mitochondrial	4	0.54	0.30	5	0.78	0.26	Etfa	1
D3Z2H9	Putative uncharacterized protein ENSMUSP00000072197	3	0.55	0.41	7	0.70	0.60		1
P08249	Malate dehydrogenase, mitochondrial	19	0.56	0.88	18	0.86	0.57	Mdh2	1
P99029	Peroxiredoxin-5, mitochondrial	3	0.57	0.83	3	0.67	0.58	Prdx5	1
Q9JII6	Alcohol dehydrogenase [NADP+]	3	0.58	0.32	3	0.85	0.75	Akr1a4	1
Q8CHP8	Phosphoglycolate phosphatase	3	0.66	0.61	3	0.93	0.62	Pgp	1
Q99LD8	N(G),N(G)-dimethylarginine dimethylaminohydrolase 2	3	1.26	1.77	4	0.56	0.71	Ddah2	1
Q00897	Alpha-1-antitrypsin 1-4	5	1.57	0.58	6	2.63	1.06	Serpina1d	2
Q9D154	Leukocyte elastase inhibitor A	3	1.58	0.99	3	2.09	0.19	Serpinb1a	2
P14602	Heat shock protein beta-1	4	1.93	0.42	3	1.59	0.76	Hspb1	2
P08228	Superoxide dismutase [Cu-Zn]	3	2.66	0.30	3	2.74	0.25	Sod1	3

endosome, a vesicular compartment that has been shown to contribute to neurite outgrowth and axon regeneration (22–24). In addition, the gene ontology cluster analysis revealed that the vesicle associate protein group was enriched and met the false discovery rate threshold 5% requirement analysis. Syntaxin13 (molecular mass of ~37 kDa), also known as syntaxin12 (accession number Q9ER00, gene name *stx12*) (Fig. 1D), was identified based on two peptides (LM(oxidation)NDFSSALN-NFQVVQR $m/z = 999.9886$ $z = 2$, and its charged state $z = 3$, and ISQATAQIK $m/z = 480.280$ $z = 2$) derived from tryptic digestion of proteins extracted from gel slices corresponding to 25–37 kDa. The peptide quantification used for the data analysis described above revealed a peak area ratio of 2.34 in KO/WT− pair, suggesting an ~2-fold increase in syntaxin13 levels in KO mice compared with WT. To validate the proteomic quantification, we analyzed syntaxin13 expression levels in neurons lacking TSC2 using a biochemical approach. We probed for syntaxin13 levels in DRG cell bodies from WT and TSC2KO mice by Western blot. The level of syntaxin13 was normalized to total α-tubulin (Fig. 2A). Extracts were also analyzed for TSC2 to test for the absence of TSC2 in TSC2KO DRG cell bodies (Fig. 2A). In TSC2KO mice, DRG cell bodies displayed about a 2-fold increase in syntaxin13 levels compared with WT (Fig. 2, A and B), consistent with our mass spectrometry analysis. We also analyzed extracts of sciatic nerve, in which DRG neurons project their axons. A residual level of TSC2 can be observed in the nerve (Fig. 2C), probably due to the presence of other cells, including Schwann cells. Similarly to the DRG cell bodies, we observed an ~2-fold increase in syntaxin13 levels. Because mTOR is genetically activated specifically in sensory neurons (6), these results suggest that the observed increase in syntaxin13 levels occurs in sensory axons.

Injury Increases Syntaxin13 Levels in the DRG Axons—Using the same biochemical approach, we then validated whether nerve injury increases syntaxin13 levels in WT DRG neurons. In contrast to the mass spectrometry data, which suggested an ~2-fold increase in syntaxin13 levels in injured WT compared with uninjured WT, we observed no significant change in syntaxin13 levels in WT DRG cell bodies following sciatic nerve injury at the four time points tested (Fig. 3, A and B). This apparent discrepancy could result from a proteomic quantification based on two peptides only. However, we observed that syntaxin13 levels increased in the sciatic nerve 24 h after injury on both the proximal and distal side (Fig. 3, C–E). This increase in syntaxin13 levels on the proximal side persists up to 4 days after injury (Fig. 3, D and E). We did not determine the levels of syntaxin13 4 days after injury on the distal side because the Wallerian degeneration process has started by that time point, and hence overall protein levels are down-regulated.

To determine whether the increase in syntaxin13 in injured nerves occurs in axons or surrounding Schwann cells, we determined the localization of syntaxin13 in longitudinal sciatic nerve sections. Immunofluorescence imaging revealed that following a 24-h crush injury, syntaxin13 localized partially with βIII-tubulin-positive axons (Fig. 4A). The ratio of syntaxin13 to βIII-tubulin levels was calculated and revealed a significant injury-induced increase in syntaxin13 levels proximal to the
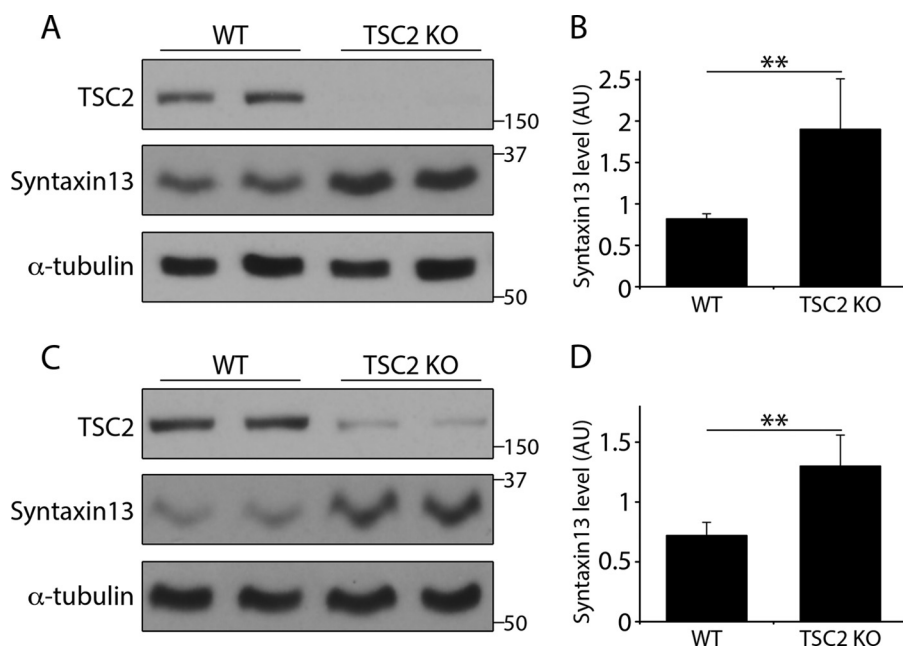
FIGURE 2. **Genetic mTOR activation increases syntaxin13 levels in DRG cell bodies and in sciatic nerve.** *A,* DRGs from WT or TSC2KO mice were analyzed by Western blot with the indicated antibodies. Duplicate samples are shown. Molecular weight is indicated on the *right side* of the Western blot panels. *B,* quantification of syntaxin13 levels normalized to α-tubulin from *A* ($n = 6$ for each genotype, mean $\pm$ S.D., **, $p < 0.01$). *C,* sciatic nerves from WT or TSC2KO mice were analyzed by Western blot with the indicated antibodies. Duplicate samples are shown. The low levels of TSC2 observed in TSC2KO sciatic nerve results from the presence of Schwann cells in the nerve. Molecular weight is indicated. *D,* quantification of syntaxin13 level normalized to α-tubulin from *C* ($n = 6$ for each genotype, mean $\pm$ S.D., **, $p < 0.01$).
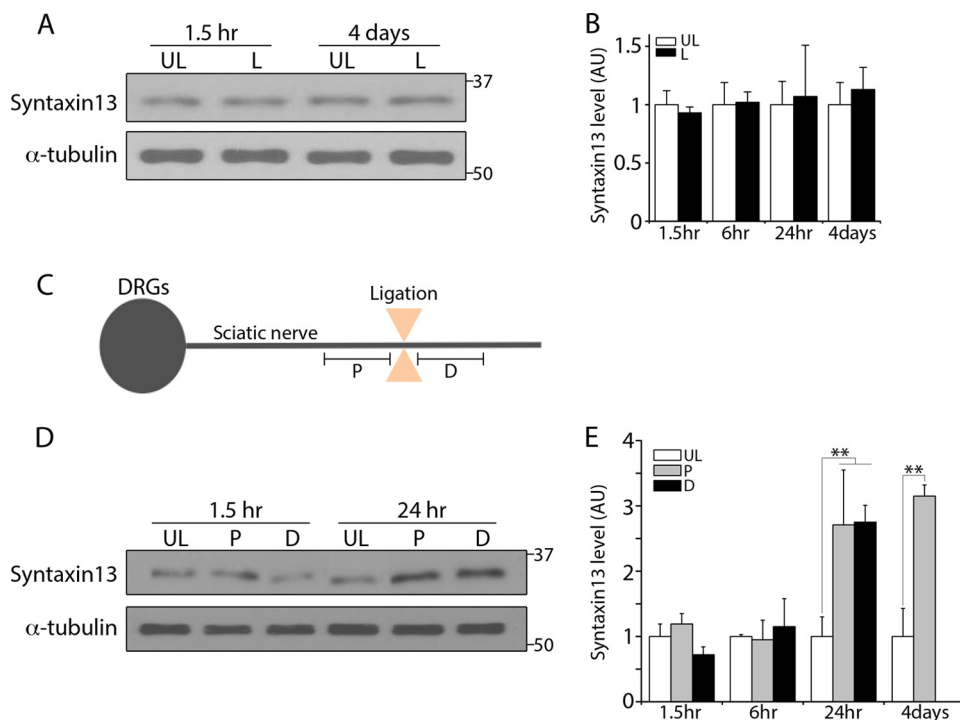

FIGURE 3. **Injury increases syntaxin13 levels in sciatic nerves.** *A,* DRGs were dissected 1.5 h or 4 days following a sciatic nerve ligation (*L*) and analyzed by Western blot with the indicated antibodies. The contralateral nerve was left unligated (*UL*) and served as a control. Molecular weight is indicated. *B,* quantification of syntaxin13 level normalized to α-tubulin from *A* ($n = 6$ for each condition, mean $\pm$ S.D.). *C,* schematic illustration of the proximal (*P*) and distal (*D*) nerve segments analyzed. *D,* proximal (*P*) and distal (*D*) segments of sciatic nerve were analyzed by Western blot with the indicated antibodies 1.5 or 24 h following a sciatic nerve ligation. The contralateral nerve was left unligated (*UL*) and served as a control. Molecular weight is indicated. *E,* quantification of syntaxin13 level normalized to α-tubulin from *C* ($n = 6$ for each condition, mean $\pm$ S.D., **, $p < 0.01$). The syntaxin13/tubulin ratio was set to 1 in the unligated samples.

injury site (Fig. 4*B*). To further confirm that injury increases syntaxin13 levels in axons, we used an *in vitro* DRG culture model, in which DRG neurons were seeded within a defined

area, allowing their axons to extend in a nearly parallel manner ("spot culture"), as described previously (Fig. 4*C*) (15, 25). DRGs were immunostained 3 h following axotomy for βIII-tubulin
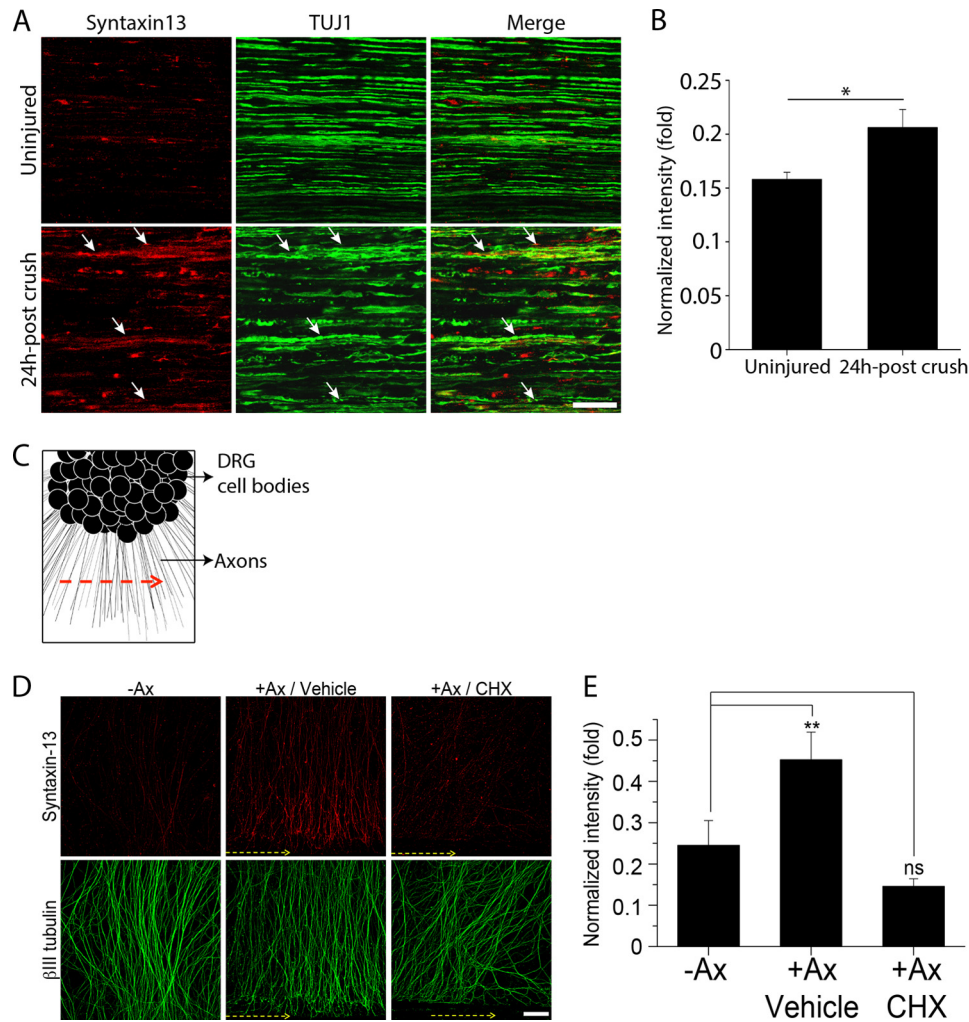
FIGURE 4. **Injury increases syntaxin13 levels in DRG axons.** *A,* longitudinal sections of sciatic nerves from WT mice without (*top panel*) or with a 24-h crush injury (*bottom panel*) were stained for syntaxin13 and βIII-tubulin (*TUJ1*). *Arrows* point to βIII-tubulin axons containing syntaxin13 on the proximal side of the crush. *Scale bar,* 200 μm. *B,* ratio of syntaxin13 to βIII-tubulin levels was calculated and revealed a significant injury-induced increase in syntaxin13 levels ($n = 9$ for each condition, mean ± S.D., *, $p < 0.05$). *C,* schematic illustration of the DRG spot culture system and the axon area analyzed. *D,* DIV7 DRG neurons were treated with cycloheximide (*CHX,* 1 mM) or vehicle (DMSO) for 1 h prior to axotomy (*Ax*), fixed, and stained for syntaxin13 and βIII-tubulin. *Scale bar,* 100 μmeters. *Yellow arrows* indicate the axotomy line. *E,* quantification of *D*. The ratio of βIII-tubulin to syntaxin13 was calculated ($n = 5$ for each condition. **, $p < 0.01$, mean ± S.D.).

and syntaxin13 (Fig. 4D). The ratio of βIII-tubulin and syntaxin13 was calculated (Fig. 4E). Axotomy increased the levels of syntaxin13 proximal to the axotomy site compare with uninjured control axons. We also tested whether this increase in syntaxin13 required protein synthesis, and we observed that in the presence of the protein synthesis inhibitor cycloheximide the level of syntaxin13 in axons was similar to nonaxotomized neurons (Fig. 4, D and E). These experiments suggest that the accumulation of syntaxin13 in injured nerve segments proximal to the injury site occurs in axons and requires protein synthesis.

Local Protein Synthesis Increases Syntaxin13 Levels in Injured Nerves—The observed increase in syntaxin13 levels in the nerve, but not in DRG cell bodies, may result from either local axonal protein synthesis at the site of injury or anterograde axonal transport of newly synthesized protein from the cell body to the site of injury. To distinguish between these two possibilities, we first tested whether inhibiting mTOR activity affected the changes in syntaxin13 levels following nerve injury. Intraperitoneal injection of rapamycin, an mTOR inhibitor, 1 h

prior to injury blocked the increase in syntaxin13 levels in nerve segments proximal to the injury site and decreased syntaxin13 levels in uninjured nerves (Fig. 5, A and B). As a control for the effectiveness of rapamycin, we observed the expected decrease in phosphorylation levels of the ribosomal protein S6 (p-S6), a known downstream target of mTOR activity required for protein synthesis (Fig. 5A). Similarly, in the presence of the protein synthesis inhibitor cycloheximide, delivered locally to the nerve, we observed reduced levels of syntaxin13 in the unligated nerve, and injury failed to increased syntaxin13 levels (Fig. 5, C and D). We then tested whether blocking axonal transport by destabilizing microtubules with nocodazole affects syntaxin13 levels. Nocodazole treatment had no significant effect on syntaxin13 levels in injured nerves (Fig. 5, E and F), whereas it decreased the levels of APP, a known anterogradely transported protein (26), used a positive control for the effectiveness of nocodazole treatment. Together with the observation that syntaxin13 mRNA is present in adult DRG axons (27), these experiments suggest that the accumulation of
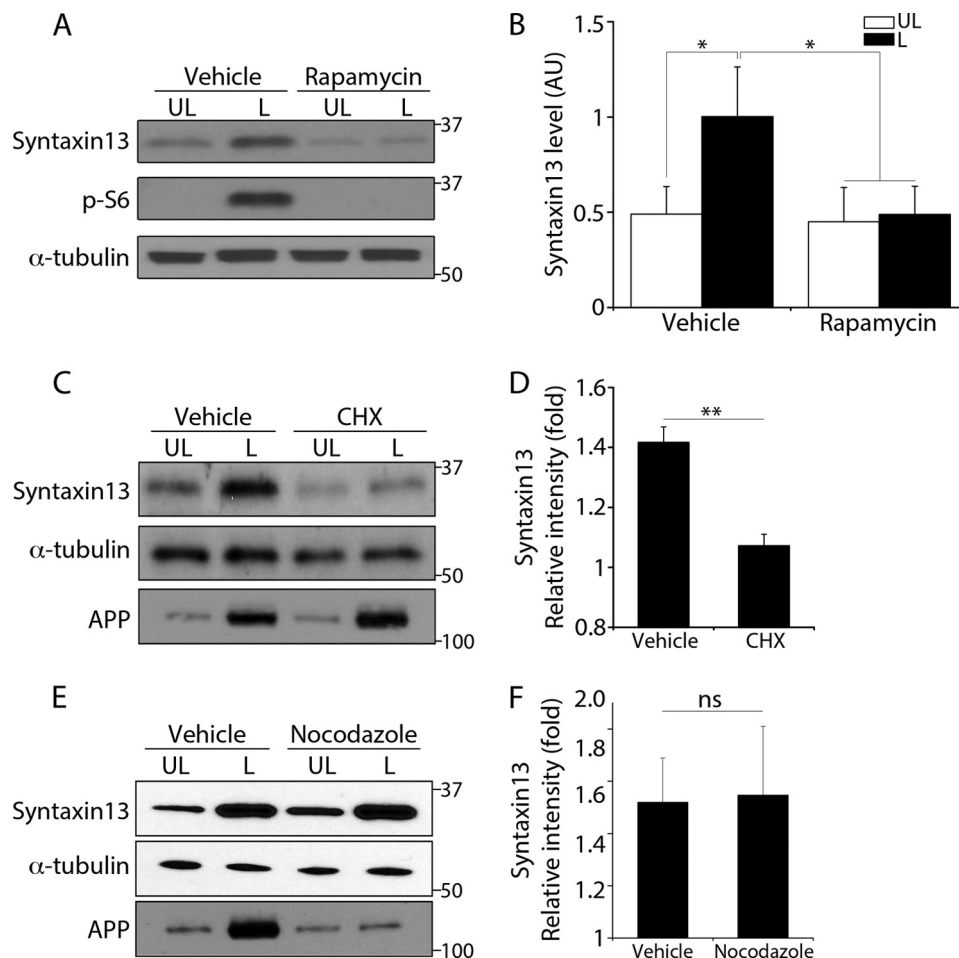
FIGURE 5. **Local protein synthesis increases syntaxin13 levels in injured nerves.** *A,* sciatic nerves were ligated in the presence of vehicle or rapamycin, and the proximal nerve segment was analyzed by Western blot 24 h later. Molecular weight is indicated. Phosphorylated ribosomal protein S6 (*p-S6*) is used as a control for the inhibitory effect of rapamycin. *B,* quantification of syntaxin13 levels normalized to α-tubulin from *A* ($n = 6$ for unligated (*UL*) and ligated (*L*) with vehicle, $n = 4$ for ligated with rapamycin, mean $\pm$ S.D., *, $p < 0.05$). *C,* sciatic nerves were ligated in the presence of vehicle or cycloheximide (*CHX*, 1 mM), and the proximal nerve segment was analyzed by Western blot 24 h later. APP is used as control for anterogradely transported molecule. Molecular weight is indicated. *D,* quantification of syntaxin13 levels normalized to α-tubulin from *C* ($n = 4$ for each condition, mean $\pm$ S.D., **, $p < 0.01$). *E,* sciatic nerves were ligated in the presence of vehicle or nocodazole, and the proximal nerve segment was analyzed by Western blot 24 h later. APP is used as control for anterogradely transported molecule. Molecular weight is indicated. *F,* quantification of syntaxin13 levels normalized to α-tubulin from *E* ($n = 4$ for each condition, mean $\pm$ S.D., *ns*, not significant).

syntaxin13 in injured nerve segments proximal to the injury site results from local protein translation.

Syntaxin13 Is Required for Axon Growth and Regeneration— The role of local protein synthesis in axon regeneration has been well established (9), and our data suggest that syntaxin13 is expressed in axons following injury. To further study the role of syntaxin13 in response to nerve injury, we first tested whether reducing syntaxin13 levels affects DRG axon growth ability. Embryonic DRG neurons were cultured and infected with lentivirus encoding scrambled shRNA control (control), syntaxin13 shRNA (KD), or syntaxin13 shRNA and GFP-syntaxin13 (KD/OE) 3 days after plating and analyzed by Western blot 4 days after infection. The levels of syntaxin13 were significantly reduced following infection with shRNA targeting syntaxin13; GFP-syntaxin13 was expressed at levels similar to that of endogenous syntaxin13 (Fig. 6A). To monitor axon growth, DRG spot cultures (15, 25) were infected with syntaxin13 shRNA or scrambled control, fixed, and stained for βIII-tubulin. When syntaxin13 was knocked down at DIV1, axon growth was severely impaired (Fig. 6, *B* and *C*), consistent with the role of syntaxin13 in neurite elongation in PC12 cells (13).

To be able to study the role of syntaxin13 in axon regeneration, we infected DRG neurons on DIV3, a time in which axons have grown up to 500 μm away from the cell body, and we performed axotomy at DIV7. We visualized axon re-growth by staining DRG neurons with βIII-tubulin after *in vitro* axotomy (Fig. 6D). In these conditions, axon growth at the time of axotomy was similar in control, syntaxin13 shRNA (KD), and syntaxin13 shRNA plus GFP-syntaxin13 (KD/OE) (Fig. 6D, *upper panel, 0 h*). To assess the regenerative capacity of injured axons, a regeneration index was calculated from the images acquired 40 h post axotomy. Axotomized axons displayed robust regeneration, whereas syntaxin13 knockdown suppressed axon regeneration (Fig. 6, *D* and *E*). GFP-syntaxin13 expression rescued the axon regeneration defects (Fig. 6, *D* and *E*). These results suggest that syntaxin13 is required to promote axon growth and regeneration in DRG neurons.
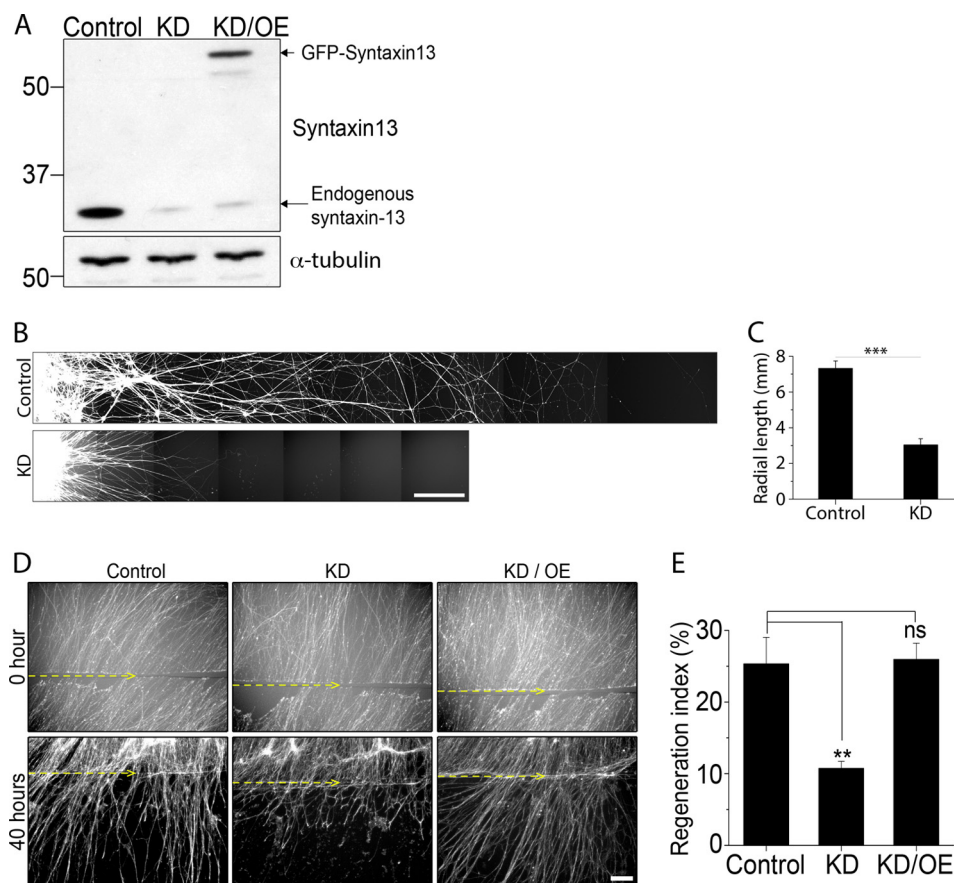
FIGURE 6. **Knockdown of syntaxin13 impairs axon growth and regeneration.** *A,* DRG neurons were infected with scramble shRNA (control), syntaxin13 shRNA (KD), or syntaxin13 shRNA and GFP-syntaxin13 (KD/OE) 3 days after plating and analyzed by Western blot 4 days after infection. Molecular weight is indicated. *B,* spot cultured embryonic DRG neurons were infected at DIV1 with control shRNA (control) or syntaxin13 shRNA (KD), fixed, and stained for βIII-tubulin at DIV7. Axon radial length was calculated. *Scale bar,* 500 μm. *C,* average radial length of *B* (*n* = 11 for each condition, mean ± S.D., ***, *p* < 0.001). *D,* to measure *in vitro* axon regeneration, DRG were infected as in *D* but at DIV3 to allow axon growth prior to *in vitro* axotomy performed at DIV7. *Control,* control shRNA; *KD,* syntaxin13 shRNA; *KD/OE,* syntaxin13 shRNA and GFP-syntaxin13. DRG were fixed and stained for βIII-tubulin 0 or 40 h after axotomy. *Yellow arrows* indicate the axotomy line. *E,* regeneration index was calculated 40 h after axotomy (*n* = 8 for each condition, mean ± S.E., **, *p* < 0.01). *ns,* not significant *Scale bar,* 100 μm.

DISCUSSION

Although mTOR has been linked to axon regeneration (6–8, 28), its downstream translational targets functioning in injured neurons have not been examined in detail. Moreover, whether mTOR plays a role locally at the injury site or distantly in the cell body remains unclear. Using a semiquantitative proteomic approach to identify proteins whose expression is regulated by injury, we show that the effect of injury correlates with the effect of genetic mTOR activation. In addition, we found that syntaxin13 expression increased in injured nerves in an mTOR-dependent manner, likely via local protein translation. Syntaxin13 is required for axon regeneration, because knockdown of syntaxin13 in cultured DRG neurons markedly reduced axon growth and regeneration, and expression of recombinant syntaxin13 rescued the axon regeneration defects. Together, these data suggest that syntaxin13 translation is regulated by mTOR in injured axons to promote axon regeneration.

Cell Body and Axonal Roles for mTOR in Axon Growth and Regeneration—The mTOR pathway has been implicated in the control of growth cone dynamics and guidance during development (29–31), axon specification, and neuronal polarity (32, 33) and axon regeneration (6–8, 28). Our previous studies showed that peripheral neurons activate mTOR in DRG cell bodies in response to injury and that this increased mTOR activity enhanced axon regeneration (6). Because mTOR and its downstream components of the translational machinery, such as P-S6K, PS6, P-4E-BP1, ribosomal-P0 and phospho-eIF-4E, are also present in axons (28, 34), mTOR activity may also contribute to the regulation of protein synthesis in adult axons.

We previously revealed that the increased level of the growth-associated protein GAP-43 following injury is dependent on mTOR activity (6). Interestingly, although GAP43 mRNA and proteins were shown to increase after nerve injury in both DRG cell body and nerve (35, 36), we found that GAP43 levels were mainly increased in the nerve. Recent work showing that only axonally targeted GAP-43 mRNA, but not cell body restricted GAP-43 mRNA, is linked to elongated axonal growth (37, 38) suggests that GAP43 axonal translation is controlled by mTOR. Similar to GAP-43, we report here that increased syntaxin13 levels in injured nerves are mediated by mTOR activity. Interestingly, syntaxin13 mRNA was recently identified as a translational target of mTOR activity (39). This study found that syntaxin13 mRNA is among the 100 transcripts whose translation is most suppressed by mTOR inhibition (39).

Together with the fact that syntaxin13 mRNA is present in adult DRG axons (27), these studies suggest that syntaxin13 is locally translated in injured axons by mTOR-dependent mechanisms to promote axon regeneration. Interestingly, the mRNAs for other members of the syntaxin family are also present in adult DRG axons (27), including syntaxin4, which is involved in lysosomal exocytosis and neurite outgrowth (40, 41). Multiple SNARE proteins may thus be locally translated following axon injury. The recent finding that localized mTOR-dependent translation of the small GTPase TC10 promotes axon growth (42) further reveals the importance of mTOR-dependent local protein synthesis in axon growth.

Axonal Protein Synthesis and Membrane Targeting—The absence of ultrastructural evidence of ribosomes in axons has raised the question as to how newly synthesized transmembrane proteins and resident endoplasmic reticulum proteins can be properly targeted to organelles and axonal membranes. Nonetheless, previous work has shown that axonally synthesized protein can successfully be targeted to membranes (43, 44). Recent work showed that after injury the neural membrane protein 35 (NMP35) is synthesized locally to increase axonal outgrowth (45). Furthermore, the NF-protocadherin, a single transmembrane protein, is translationally regulated in retinal growth cones (46). The presence of vesicular endoplasmic reticulum proteins suggests that a functional equivalent of the rough endoplasmic reticulum and Golgi complex exists in axonal compartments (47) and may account for targeting newly synthesized protein to membranes. Indeed, axons possess components of endoplasmic reticulum and Golgi and are capable of local protein (48) and lipid synthesis (49). Merianda *et al.* (48) also report that inhibition of Golgi function in isolated adult DRG axons attenuates translation-dependent axon growth responses and that the capacity for secreting locally synthesized proteins in axons appears to be increased by injury. Similarly to the local translation of NMP35, our results suggest that local translation of syntaxin13 following injury is required for axon growth.

Syntaxin 13 and the Recycling Endosome in Axon Growth and Regeneration—Membrane trafficking pathways and especially endocytosis are important for neurite outgrowth and guidance during development (22–24, 50, 51). Syntaxin13 localizes to recycling endosomes where it functions to recycle plasma membrane constituents (11, 13, 52). Conceivably, injury-induced increase of syntaxin13 levels may promote more efficient recycling of integrins, which enhance sensory axon regeneration by being transported in distinct recycling endosomal cargoes (53–55). Because syntaxin13 was shown to localize to bi-directionally moving recycling endosomes in hippocampal axons (56) and peripheral sensory axons (57), it will be interesting to determine whether integrin recycling requires syntaxin13 function.

Syntaxin13 could also play a role in resealing cut axons following axotomy, a process that requires both exo- and endocytic events (23). Resealing requires vesicle fusion with the plasma membrane, a process supported by an interaction between the calcium-sensing synaptotagmin and the SNARE machinery. As an endosomal SNARE, syntaxin13 may have a role in this process as well.

Injury signaling is another important regulator of the neuronal response to injury (10). Syntaxin13 localizes to bi-directional endosomes carrying the scaffolding protein JIP3 on their surface (57), and JIP3 retrograde transport has been implicated in the regenerative response (58, 59).

Finally, syntaxin13 may play a role in controlling local signaling pathways induced by injury. Given that endocytic organelles can play an active role in signal propagation and amplification (60), perturbation of the endocytic pathway by syntaxin13 levels may lead to decreased growth ability via the alteration of essential signaling pathways. Further studies will be needed to determine the molecular mechanisms that syntaxin13 utilizes to promote growth and regeneration of axons.

REFERENCES

1. Liu, K., Tedeschi, A., Park, K. K., and He, Z. (2011) Neuronal intrinsic mechanisms of axon regeneration. *Annu. Rev. Neurosci.* **34,** 131–152
2. Lieberman, A. R. (1971) The axon reaction: a review of the principal features of perikaryal responses to axon injury. *Int. Rev. Neurobiol.* **14,** 49–124
3. Cragg, B. G. (1970) What is the signal for chromatolysis? *Brain Res.* **23,** 1–21
4. Watson, W. E. (1968) Observations on the nucleolar and total cell body nucleic acid of injured nerve cells. *J. Physiol.* **196,** 655–676
5. Watson, W. E. (1969) The change in dry mass of hypoglassal neurones induced by puromycin, and the effects of nerve injury. *J. Physiol.* **201,** 80P–81P
6. Abe, N., Borson, S. H., Gambello, M. J., Wang, F., and Cavalli, V. (2010) Mammalian target of rapamycin (mTOR) activation increases axonal growth capacity of injured peripheral nerves. *J. Biol. Chem.* **285,** 28034–28043
7. Park, K. K., Liu, K., Hu, Y., Smith, P. D., Wang, C., Cai, B., Xu, B., Connolly, L., Kramvis, I., Sahin, M., and He, Z. (2008) Promoting axon regeneration in the adult CNS by modulation of the PTEN/mTOR pathway. *Science* **322,** 963–966
8. Liu, K., Lu, Y., Lee, J. K., Samara, R., Willenberg, R., Sears-Kraxberger, I., Tedeschi, A., Park, K. K., Jin, D., Cai, B., Xu, B., Connolly, L., Steward, O., Zheng, B., and He, Z. (2010) PTEN deletion enhances the regenerative ability of adult corticospinal neurons. *Nat. Neurosci.* **13,** 1075–1081
9. Gumy, L. F., Tan, C. L., and Fawcett, J. W. (2010) The role of local protein synthesis and degradation in axon regeneration. *Exp. Neurol.* **223,** 28–37
10. Rishal, I., and Fainzilber, M. (2014) Axon-soma communication in neuronal injury. *Nat. Rev. Neurosci.* **15,** 32–42
11. Prekeris, R., Klumperman, J., Chen, Y. A., and Scheller, R. H. (1998) Syntaxin 13 mediates cycling of plasma membrane proteins via tubulovesicular recycling endosomes. *J. Cell Biol.* **143,** 957–971
12. Skalski, M., Yi, Q., Kean, M. J., Myers, D. W., Williams, K. C., Burtnik, A., and Coppolino, M. G. (2010) Lamellipodium extension and membrane ruffling require different SNARE-mediated trafficking pathways. *BMC Cell Biol.* **11,** 62
13. Hirling, H., Steiner, P., Chaperon, C., Marsault, R., Regazzi, R., and Catsicas, S. (2000) Syntaxin 13 is a developmentally regulated SNARE involved in neurite outgrowth and endosomal trafficking. *Eur. J. Neurosci.* **12,** 1913–1923
14. Deleted in proof

15. Cho, Y., and Cavalli, V. (2012) HDAC5 is a novel injury-regulated tubulin deacetylase controlling axon regeneration. *EMBO J.* **31,** 3063–3078

16. Chalkley, R. J., Baker, P. R., Medzihradszky, K. F., Lynn, A. J., and Burlingame, A. L. (2008) In-depth analysis of tandem mass spectrometry data from disparate instrument types. *Mol. Cell. Proteomics* **7,** 2386–2398

17. Clauser, K. R., Baker, P., and Burlingame, A. L. (1999) Role of accurate mass measurement ($+/-$ 10 ppm) in protein identification strategies employing MS or MS/MS and database searching. *Anal. Chem.* **71,** 2871–2882

18. Guan, S., Price, J. C., Prusiner, S. B., Ghaemmaghami, S., and Burlingame, A. L. (2011) A data processing pipeline for mammalian proteome dynamics studies using stable isotope metabolic labeling. *Mol. Cell. Proteomics* **10,** M111.010728

19. Salvador, S., and Chan, P. (2004) *Proceedings of the 16th IEEE International Conference on Tools with Artificial Intelligence*, IEEE Computer Society, pp. 576–584, Washington, D. C.

20. MacKay, D. J. C. (2003) *Information Theory, Inference and Learning Algorithms*, pp. 284–310, Cambridge University Press

21. Kopp, M. A., Liebscher, T., Niedeggen, A., Laufer, S., Brommer, B., Jungehulsing, G. J., Strittmatter, S. M., Dirnagl, U., and Schwab, J. M. (2012) Small-molecule-induced Rho-inhibition: NSAIDs after spinal cord injury. *Cell Tissue Res.* **349,** 119–132

22. Sann, S., Wang, Z., Brown, H., and Jin, Y. (2009) Roles of endosomal trafficking in neurite outgrowth and guidance. *Trends Cell Biol.* **19,** 317–324

23. Tuck, E., and Cavalli, V. (2010) Roles of membrane trafficking in nerve repair and regeneration. *Commun. Integr. Biol.* **3,** 209–214

24. Winckler, B., and Yap, C. C. (2011) Endocytosis and endosomes at the crossroads of regulating trafficking of axon outgrowth-modifying receptors. *Traffic* **12,** 1099–1108

25. Cho, Y., Sloutsky, R., Naegle, K. M., and Cavalli, V. (2013) Injury-induced HDAC5 nuclear export is essential for axon regeneration. *Cell* **155,** 894–908

26. Koo, E. H., Sisodia, S. S., Archer, D. R., Martin, L. J., Weidemann, A., Beyreuther, K., Fischer, P., Masters, C. L., and Price, D. L. (1990) Precursor of amyloid protein in Alzheimer disease undergoes fast anterograde axonal transport. *Proc. Natl. Acad. Sci. U.S.A.* **87,** 1561–1565

27. Gumy, L. F., Yeo, G. S., Tung, Y. C., Zivraj, K. H., Willis, D., Coppola, G., Lam, B. Y., Twiss, J. L., Holt, C. E., and Fawcett, J. W. (2011) Transcriptome analysis of embryonic and adult sensory axons reveals changes in mRNA repertoire localization. *RNA* **17,** 85–98

28. Verma, P., Chierzi, S., Codd, A. M., Campbell, D. S., Meyer, R. L., Holt, C. E., and Fawcett, J. W. (2005) Axonal protein synthesis and degradation are necessary for efficient growth cone regeneration. *J. Neurosci.* **25,** 331–342

29. Nie, D., Di Nardo, A., Han, J. M., Baharanyi, H., Kramvis, I., Huynh, T., Dabora, S., Codeluppi, S., Pandolfi, P. P., Pasquale, E. B., and Sahin, M. (2010) Tsc2-Rheb signaling regulates EphA-mediated axon guidance. *Nat. Neurosci.* **13,** 163–172

30. Wu, K. Y., Hengst, U., Cox, L. J., Macosko, E. Z., Jeromin, A., Urquhart, E. R., and Jaffrey, S. R. (2005) Local translation of RhoA regulates growth cone collapse. *Nature* **436,** 1020–1024

31. Campbell, D. S., and Holt, C. E. (2001) Chemotropic responses of retinal growth cones mediated by rapid local protein synthesis and degradation. *Neuron* **32,** 1013–1026

32. Choi, Y. J., Di Nardo, A., Kramvis, I., Meikle, L., Kwiatkowski, D. J., Sahin, M., and He, X. (2008) Tuberous sclerosis complex proteins control axon formation. *Genes Dev.* **22,** 2485–2495

33. Wildonger, J., Jan, L. Y., and Jan, Y. N. (2008) The Tsc1-Tsc2 complex influences neuronal polarity by modulating TORC1 activity and SAD levels. *Genes Dev.* **22,** 2447–2453

34. Jiménez-Díaz, L., Géranton, S. M., Passmore, G. M., Leith, J. L., Fisher, A. S., Berliocchi, L., Sivasubramaniam, A. K., Sheasby, A., Lumb, B. M., and Hunt, S. P. (2008) Local translation in primary afferent fibers regulates nociception. *PLoS One* **3,** e1961

35. Schreyer, D. J., and Skene, J. H. (1993) Injury-associated induction of GAP-43 expression displays axon branch specificity in rat dorsal root ganglion neurons. *J. Neurobiol.* **24,** 959–970

36. Van der Zee, C. E., Nielander, H. B., Vos, J. P., Lopes da Silva, S., Verhaagen, J., Oestreicher, A. B., Schrama, L. H., Schotman, P., and Gispen, W. H. (1989) Expression of growth-associated protein B-50 (GAP43) in dorsal root ganglia and sciatic nerve during regenerative sprouting. *J. Neurosci.* **9,** 3505–3512

37. Yoo, S., Kim, H. H., Kim, P., Donnelly, C. J., Kalinski, A. L., Vuppalanchi, D., Park, M., Lee, S. J., Merianda, T. T., Perrone-Bizzozero, N. I., and Twiss, J. L. (2013) A HuD-ZBP1 ribonucleoprotein complex localizes GAP-43 mRNA into axons through its 3′ untranslated region AU-rich regulatory element. *J. Neurochem.* **126,** 792–804

38. Donnelly, C. J., Park, M., Spillane, M., Yoo, S., Pacheco, A., Gomes, C., Vuppalanchi, D., McDonald, M., Kim, H. H., Kim, H. K., Merianda, T. T., Gallo, G., and Twiss, J. L. (2013) Axonally synthesized β-actin and GAP-43 proteins support distinct modes of axonal growth. *J. Neurosci.* **33,** 3311–3322

39. Thoreen, C. C., Chantranupong, L., Keys, H. R., Wang, T., Gray, N. S., and Sabatini, D. M. (2012) A unifying model for mTORC1-mediated regulation of mRNA translation. *Nature* **485,** 109–113

40. Rao, S. K., Huynh, C., Proux-Gillardeaux, V., Galli, T., and Andrews, N. W. (2004) Identification of SNAREs involved in synaptotagmin VII-regulated lysosomal exocytosis. *J. Biol. Chem.* **279,** 20471–20479

41. Arantes, R. M., and Andrews, N. W. (2006) A role for synaptotagmin VII-regulated exocytosis of lysosomes in neurite outgrowth from primary sympathetic neurons. *J. Neurosci.* **26,** 4630–4637

42. Gracias, N. G., Shirkey-Son, N. J., and Hengst, U. (2014) Local translation of TC10 is required for membrane expansion durign axon outgrowth. *Nat. Commun.* 10.1038/ncomms4506

43. Spencer, G. E., Syed, N. I., van Kesteren, E., Lukowiak, K., Geraerts, W. P., and van Minnen, J. (2000) Synthesis and functional integration of a neurotransmitter receptor in isolated invertebrate axons. *J. Neurobiol.* **44,** 72–81

44. Brittis, P. A., Lu, Q., and Flanagan, J. G. (2002) Axonal protein synthesis provides a mechanism for localized regulation at an intermediate target. *Cell* **110,** 223–235

45. Merianda, T. T., Vuppalanchi, D., Yoo, S., Blesch, A., and Twiss, J. L. (2013) Axonal transport of neural membrane protein 35 mRNA increases axon growth. *J. Cell Sci.* **126,** 90–102

46. Leung, L. C., Urbančič, V., Baudet, M. L., Dwivedy, A., Bayley, T. G., Lee, A. C., Harris, W. A., and Holt, C. E. (2013) Coupling of NF-protocadherin signaling to axon guidance by cue-induced translation. *Nat. Neurosci.* **16,** 166–173

47. Willis, D., Li, K. W., Zheng, J. Q., Chang, J. H., Smit, A. B., Smit, A., Kelly, T., Merianda, T. T., Sylvester, J., van Minnen, J., and Twiss, J. L. (2005) Differential transport and local translation of cytoskeletal, injury-response, and neurodegeneration protein mRNAs in axons. *J. Neurosci.* **25,** 778–791

48. Merianda, T. T., Lin, A. C., Lam, J. S., Vuppalanchi, D., Willis, D. E., Karin, N., Holt, C. E., and Twiss, J. L. (2009) A functional equivalent of endoplasmic reticulum and Golgi in axons for secretion of locally synthesized proteins. *Mol. Cell. Neurosci.* **40,** 128–142

49. Vance, J. E., Campenot, R. B., and Vance, D. E. (2000) The synthesis and transport of lipids for axonal growth and nerve regeneration. *Biochim. Biophys. Acta* **1486,** 84–96

50. Prager-Khoutorsky, M., and Spira, M. E. (2009) Neurite retraction and regrowth regulated by membrane retrieval, membrane supply, and actin dynamics. *Brain Res.* **1251,** 65–79

51. Futerman, A. H., and Banker, G. A. (1996) The economics of neurite outgrowth–the addition of new membrane to growing axons. *Trends Neurosci.* **19,** 144–149

52. Jahn, R., and Scheller, R. H. (2006) SNAREs– engines for membrane fusion. *Nat. Rev. Mol. Cell Biol.* **7,** 631–643

53. Andrews, M. R., Czvitkovich, S., Dassie, E., Vogelaar, C. F., Faissner, A., Blits, B., Gage, F. H., ffrench-Constant, C., and Fawcett, J. W. (2009) α9 integrin promotes neurite outgrowth on tenascin-C and enhances sensory axon regeneration. *J. Neurosci.* **29,** 5546–5557

54. Eva, R., Crisp, S., Marland, J. R., Norman, J. C., Kanamarlapudi, V., ffrench-Constant, C., and Fawcett, J. W. (2012) ARF6 directs axon transport and traffic of integrins and regulates axon growth in adult DRG neurons. *J. Neurosci.* **32,** 10352–10364

55. Eva, R., Dassie, E., Caswell, P. T., Dick, G., ffrench-Constant, C., Norman, J. C., and Fawcett, J. W. (2010) Rab11 and its effector Rab coupling protein contribute to the trafficking of β1 integrins during axon growth in adult dorsal root ganglion neurons and PC12 cells. *J. Neurosci.* **30,** 11654–11669

56. Prekeris, R., Foletti, D. L., and Scheller, R. H. (1999) Dynamics of tubulovesicular recycling endosomes in hippocampal neurons. *J. Neurosci.* **19,** 10324–10337

57. Abe, N., Almenar-Queralt, A., Lillo, C., Shen, Z., Lozach, J., Briggs, S. P., Williams, D. S., Goldstein, L. S., and Cavalli, V. (2009) Sunday driver interacts with two distinct classes of axonal organelles. *J. Biol. Chem.* **284,** 34628–34639

58. Cavalli, V., Kujala, P., Klumperman, J., and Goldstein, L. S. (2005) Sunday driver links axonal transport to damage signaling. *J. Cell Biol.* **168,** 775–787

59. Shin, J. E., Cho, Y., Beirowski, B., Milbrandt, J., Cavalli, V., and DiAntonio, A. (2012) Dual leucine zipper kinase is required for retrograde injury signaling and axonal regeneration. *Neuron* **74,** 1015–1022

60. Miaczynska, M., Pelkmans, L., and Zerial, M. (2004) Not just a sink: endosomes in control of signal transduction. *Curr. Opin. Cell Biol.* **16,** 400–406